THE JOURNAL OF PHYSICAL CHEMISTRY Letters

Letter

pubs.acs.org/JPCL

Dipolar Nanodomains in Protein Hydration Shells

Daniel R. Martin[†] and Dmitry V. Matyushov*[,†,‡]

[†]Department of Physics and [‡]Department of Chemistry & Biochemistry, Arizona State University, P.O. Box 871504, Tempe, Arizona 85287, United States

Supporting Information

ABSTRACT: The network of hydrogen bonds characteristic of bulk water is significantly disturbed at the protein−water interface, where local fields induce mutually frustrated dipolar domains with potentially novel structure and dynamics. Here the dipolar susceptibility of hydration shells of lysozyme is studied by molecular dynamics simulations in a broad range of temperatures, 140−300 K. The real part of the susceptibility passes through a broad maximum as a function of temperature. The maximum shifts to higher temperatures with increasing frequency of the dielectric experiment. This phenomenology is consistent with that reported for bulk relaxor ferroelectrics, where it is related to the formation of dipolar nanodomains. Nanodomains in the hydration shell extend 12−15 Å from the protein surface into the bulk. Their dynamics are significantly slower than the dynamics of bulk water. The domains dynamically freeze into a ferroelectric glass below 160 K, at which point the Arrhenius plot of the dipolar relaxation time becomes significantly steeper.

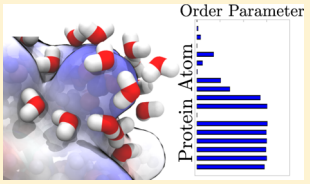

Solubility and folding stability of proteins in water require the presence of a large number of ionized residues at the protein's surface. These ionized residues provide the solubility or folding stabilization free energy but also significantly influence the hydration shell.[1] With ≃500 water molecules in only the first hydration layer of a typical globular protein, there is a large number of microscopic configurations of the shell. One can therefore think of the hydration shell as a separate subensemble with properties potentially distinct from bulk water. The purpose of this communication is to study this perspective by molecular dynamics (MD) simulations. In particular, the orientational and density profiles of the shell are compared in a broad range of temperatures. We find that orientations of the shell waters are highly correlated, and these correlations are best described in terms of dipolar domains with phenomenology similar to that reported for bulk relaxor ferroelectrics.[2,3]

The interactions of the surface water molecules with the protein are often stronger than the water−water interactions in the bulk,[4] in particular, when double hydrogen bonds between water and protein are allowed.[5] These strong surface forces break the bulk-like network of hydrogen bonds and produce a new orientational structure of the interfacial water.[6] The hydration shell shows the presence of both highly cooperative and highly disordered domains.[7,8] The question addressed here is how to characterize these domains.

It is well-established that interfacial water molecules predominantly orient parallel to an extended hydrophobic surface[9] but align along the electrostatic field produced by surface charges.[10,11] What we do not know is whether the protein−water interface follows these two distinct scenarios, or, alternatively, the configurational space is not sufficient to allow both hydrophobic and field-dictated orientational patterns to coexist. Our present results indicate that only field-induced orientations are established. No indication of the hydrophobic orientational scenario is found; the water molecules are mostly disordered between the regions of strong field-promoted alignment.

The next question is whether the orientational structure of the interfacial water may result in new observable properties of protein hydration shells, which consequently could be distinguished as a distinct "biological water".[12] The main question here is whether the statistics and dynamics of interfacial dipoles are mostly single-particle, as caused by the breakdown of the hydrogen bonding structure present in the bulk, or, alternatively, some extent of cooperativity distinct from the bulk builds up. In the latter case, thermal excitations of the shell are better described as collective motions of strongly correlated dipolar domains.[13] One can make even one step further and imagine a possibility of a separate mesophase in the hydration shell. This scenario might occur by the interfacial stabilization of a phase existing only as a metastable local minimum on the free-energy landscape of the bulk phase.[14]

There is evidence that some of these scenarios might be realized in hydration shells of proteins.[7,15−17] The residence dynamics[18] or, alternatively, the dynamics of the number of first-shell water molecules, are highly dispersive. It combines short, in picoseconds, with long, in nanoseconds, relaxation times. This observation, as well as other evidence,[1,4,5] points to the presence of water molecules strongly attached to the protein, along with many water molecules with their dynamics only slightly slower[19] or even faster than in the bulk, depending on hydrophilicity.[20] The overall dynamical heterogeneity is a distinctive signature of the protein hydration shell.

The depth of water shell perturbed by the protein strongly depends on whether the interfacial density or orientational

Received: December 2, 2014
Accepted: January 14, 2015
Published: January 14, 2015

DOI: 10.1021/jz5025433
J. Phys. Chem. Lett. 2015, 6, 407−412

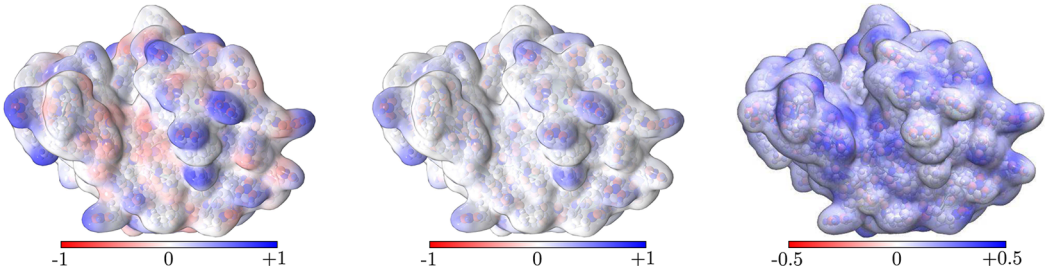

Figure 1. Map of p_1 (left panel), p_2 (central panel), and p_{21} (right panel) order parameters of water dipoles in the hydration shell of lysozyme at 300 K (a = 3 Å). The protein atoms are labeled according to their partial charges, blue for positive and red for negative. The maps are calculated by averaging the order parameters over 20 ns of MD simulations.

structure are concerned. The typical ∼15% enhancement of the interfacial density is relatively short-ranged and is limited to the first hydration layer.[21] Most of this enhancement comes from purely geometrical and topological[7] effects of the solute−solvent packing, with some additional density enhancement promoted by negative surface groups.[10] On the contrary, the perturbation of the water orientations is long-ranged and often propagates three to five hydration layers into the bulk.[22,23] Long-range perturbations of the water orientational structure are not limited to proteins and have been observed for many interfaces.[24,25] The question here is what are the observable signatures of such long-range perturbations[22,23] and whether the terminology of correlated domains[16] describes the hydration shell best. In terms of the interfacial dynamics, the question is whether the surface defects characterized by locally slow dynamics can merge into cooperative domains[13] with long relaxation times, in the range of nanoseconds, as is often recorded by the Stokes shift dynamics of spectroscopic probes.[26]

In a search for observable consequences of domain formation, one naturally turns to the temperature variation as a means to probe the statistics and dynamics of the shell dipoles. One is helped here by the well-established phenomenology of relaxor ferroelectrics.[2,3] These materials display a number of properties attributed to cooperative dipolar nanodomains. Among them is a strong increase in the dielectric constant with lowering temperature. The dielectric constant of a relaxor ferroelectric does not reach the Curie point of the ferroelectric transition but instead drops at a glass-transition temperature when dipolar domains dynamically freeze on the time of observation. The dynamical nature of the transition is confirmed by the dispersion of the maximum, which shifts to higher temperatures with increasing frequency of the dielectric experiment.[3] We look here for a similar phenomenology in simulations of hydrated lysozyme at a number of temperatures. We indeed find many parallels to relaxor ferroelectrics. There is a dispersive maximum of the real part of the shell dipolar susceptibility versus temperature, which shifts to higher temperatures at higher frequencies. The shell nanodomains freeze into a glass with a nonzero residual polarization (ferroelectric glass) at $T \simeq 140-160$ K, commonly associated with the glass-transition temperature of hydrated proteins.[27]

The MD simulations of lysozyme hydrated in TIP3P water were done with the use of NAMD software package.[28] The details of the simulation protocol are given in the Supporting Information (SI). Here we focus on the results. Overall, the results reported here have required 1.8 μs of MD trajectories for 12 different temperatures. The simulation cell contained one lysozyme protein hydrated by 27 673 water molecules.

We start characterizing the orientational structure of the hydration layer with the first, p_1, and second-order, p_2, orientational order parameters. They are calculated for a shell of thickness a = 3 Å surrounding the van der Waals surface of the protein.[6] p_1 is defined as the average projection of the unit vector $\hat{\mathbf{m}}(\mathrm{r})$ of the water dipole moment on the unit vector $\hat{\mathbf{n}}(\mathrm{r})$ connecting the water oxygen to the protein atom closest to it, $p_1(\mathbf{r}) = \langle \cos \theta_w(\mathbf{r}) \rangle$, where $\cos \theta_w(\mathbf{r}) = \hat{\mathbf{m}}(\mathbf{r})\cdot\hat{\mathbf{n}}(\mathbf{r})$ and $\mathbf{r}$ is the oxygen coordinate within the 3 Å shell. The calculations are performed using a part (20 ns) of the simulation trajectory. (See the SI for more detail.) The resulting map of p_1 is shown in the left panel of Figure 1. The middle panel in Figure 1 shows the second-order orientational order parameter $p_2(\mathbf{r}) = \langle 3[\cos \theta_w(\mathbf{r})]^2 - 1) \rangle/2$.

The coincidental blue regions of p_1 and p_2 represent water molecules oriented largely outward from the dividing surface, along the field produced by positively charged protein residues. The negatively charged residues produce regions of negative p_1, with the water dipoles directed toward the dividing surface. However, the order parameter p_2 gets mostly white coloring in those regions, suggesting that the strictly inward orientation of the dipole, requiring two dangling or two H-bonded protons,[29] is not realized. Instead, the most probable angle between the dipole and the surface normal is ≃125°.

A more detailed picture of orientations of two OH bonds for a given orientation of the water dipole can be gained from an additional order parameter, $p_{21}(\mathbf{r}) = (1/2)\langle [\sin \theta_w(\mathbf{r})]^2 \cos 2\chi_w(\mathbf{r}) \rangle$. This order parameter arises, in addition to p_1 and p_2, from the expansion of the interfacial molecular orientations in rotational invariants.[30] The angle $\chi_w(\mathbf{r})$ is between the plane of the water molecule and the plane containing the water dipole moment $\hat{\mathbf{m}}(\mathrm{r})$ and the normal unit vector $\hat{\mathbf{n}}(\mathrm{r})$. The presence of the OH bond pointing toward the solute when the dipole moment is along the dividing surface ($\theta_w \simeq \pi/2$) results in $\cos(2\chi_w) \simeq 1$ and p_{21} approaching 1/2. Correspondingly, when the water plane is perpendicular to the plane formed by the dipole moment and the surface normal, $\cos(2\chi_w) \simeq -1$ and p_{21} is close to −1/2. The first observation is that this latter scenario is never realized. It implies that one of the interfacial protons always points to the bulk to saturate hydrogen bonds with other water molecules. Comparing the red colored regions of the p_1 map with the corresponding regions of p_2 and p_{21}, one sees that only one OH bond points toward the protein for waters close to the negative residues. Finally, there are regions where both p_1 and p_2 gain white coloring, corresponding to essentially random orientations of interfacial waters. This analysis clearly shows that only field-dictated and disordered dipolar orientations are realized in the hydration shell. Very few dipoles parallel to the dividing surface, as expected for extended

DOI: 10.1021/jz5025433
J. Phys. Chem. Lett. 2015, 6, 407−412

hydrophobic surfaces,[9] can be observed. Some of the quantitative parts of this picture might change depending on the water model used (with a greater symmetry of the p_{21} map for more symmetric water models, such as TIP5P[31]), but the general phenomenology is robust.

The unusual properties of the hydration shell are displayed by the temperature dependence of the shell dipolar susceptibility (Figure 2a)

$$\chi_M(a) = \frac{1}{3\nu_w k_B T} \frac{\langle (\delta \mathbf{M}_s(a, 0))^2 \rangle}{\langle N_s(a) \rangle} \quad (1)$$

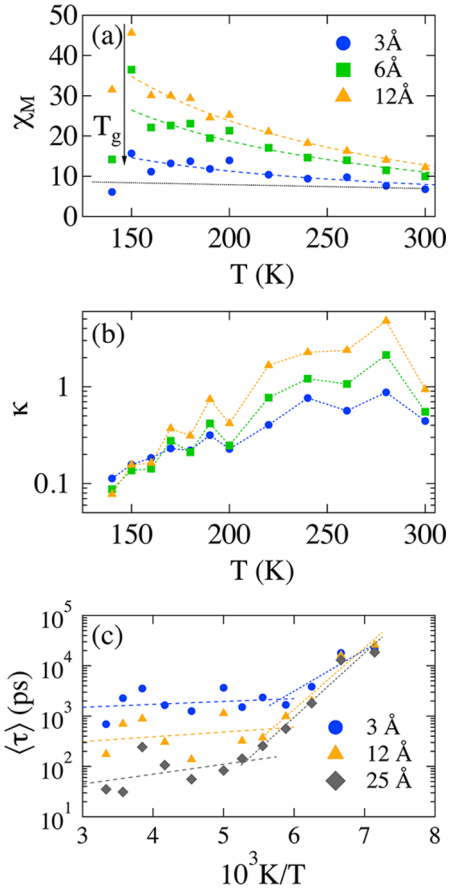

Figure 2. (a) First-shell dipolar susceptibility $\chi_M(a)$ (eq 1) versus T for shell thickness a indicated in the plot. The dotted line shows the temperature dependence of the dipolar susceptibility consistent with the temperature variation of the dielectric constant of water, $(\partial \epsilon_s/\partial T)_P = -0.12\ K^{-1}$. The short-dashed lines are fits of the simulation points to functions linear in $1/T$; the vertical arrow indicates the glass-transition temperature at which the hydration shell freezes into a ferroelectric glass. (b) Compressibility, $\kappa = \langle (\delta N_s(a))^2 \rangle / \langle N_s(a) \rangle$; the coloring of the points corresponds to the shell thickness a, as indicated in panel a. The dotted lines connect the points. (c) Average relaxation time of the shell dipole moment (eq 2) versus inverse temperature for the shell sizes indicated in the plot. The dashed lines are the Arrhenius fits.

Here $\mathbf{M}_s(a, t)$ is the instantaneous dipole moment of the shell and $\delta \mathbf{M}_s(a, t)$ is the deviation of the shell dipole at time t from its average value. It is calculated by summing up all water dipoles within the shell of thickness a surrounding the van der Waals surface of the protein; the average is taken along the simulation trajectory. In addition, $\nu_w = (\pi/6)\sigma_w^3$, $\sigma_w = 2.87$ Å is the volume of a single water molecule, and $\langle N_s(a) \rangle$ is the average number of water molecules in the shell.

The observed temperature dependence of the dipolar susceptibility is stronger than expected from the fluctuation–dissipation theorem predicting $\langle (\delta \mathbf{M}_s(a, 0))^2 \rangle \propto T$. From this relation, $\chi_M(a)$ in eq 1 should be nearly temperature-independent, but a strong increase in $\chi_M(a)$ with lowering temperature is observed instead, also stronger than what is anticipated from the dielectric constant of bulk water (dotted line in Figure 2a).[32] Fluctuations of the shell density show the behavior essentially opposite to the shell dipole. The variance of the number of first-shell water molecules, $\langle (\delta N_s(a))^2 \rangle$, grows with temperature, and the shell compressibility, defined as $\kappa = \langle (\delta N_s(a))^2 \rangle / \langle N_s(a) \rangle$,[33] increases by nearly an order of magnitude in the temperature range 140–300 K studied by simulations (Figure 2b). There is therefore a clear contrast between increasing fluctuations of the water dipoles and decreasing fluctuations of the water density when the temperature is lowered. These two results are in fact consistent with the expectation that a more rigid shell at lower temperatures will not be constantly disrupted by density fluctuations and will trigger growing dipolar domains.

The temperature dependence of the shell dipolar susceptibility is analogous to similar phenomenology found for bulk relaxor ferroelectrics.[2,3] In these materials random crystalline defects are responsible for the formation of polar nanodomains, which are prevented, by disorder, from forming a regular ferroelectric crystal. Charge impurities in such materials are the source of random local fields inducing the domain formation. An analogy to the protein–water interface cannot be missed here. A nearly uniform distribution of oppositely charged surface residues[34] creates random pinning sites at the protein surface. They both preferentially orient the water molecules in each domain and prevent the domains' growth beyond the size restricted by the average distance between the charged surface residues. The domains can grow into the bulk, but significant growth cannot be realized without support of uniformly charged regions of the protein.

In agreement with the phenomenology of relaxor ferroelectrics,[3] we observe a dynamical freezing of the hydration shell, at $T < 160$ K, into a state with a nonzero net polarization and a significantly reduced variance of the dipole moment (marked by T_g in Figure 2a). Because the freezing is dynamic, which is observed when the observation time (the length of the simulation trajectory) falls below the relaxation time of the interfacial domains, a significant frequency dispersion of the susceptibility is expected.[3] Figure 3 shows the real part, $\chi'_M(\omega,T)$, of the frequency-dependent susceptibility $\chi_M(\omega,T)$ against temperature. The results are remarkably similar to experimentally reported frequency dispersive maxima of the dielectric constant of relaxor ferroelectrics. Specifically, the maximum of $\chi'_M(T)$ shifts to a higher temperature with increasing frequency ω because dynamical freezing of nanodomains is realized when the condition $\omega\tau_M(T) \simeq 1$ is reached.[3] Here $\tau_M(T)$ is the relaxation time of the shell dipole shown in Figure 2c. It is calculated from the time autocorrelation function of the dipole moment according to the equation

$$\tau_M(a) = [\langle (\delta \mathbf{M}_s(a, 0))^2 \rangle]^{-1} \int_0^\infty \langle \delta \mathbf{M}_s(a, t) \cdot \delta \mathbf{M}_s(a, 0) \rangle \, dt \quad (2)$$

DOI: 10.1021/jz5025433
J. Phys. Chem. Lett. 2015, 6, 407–412

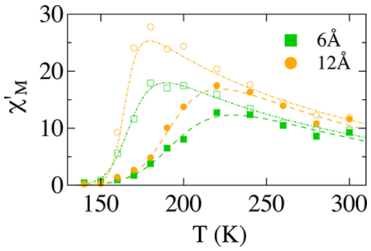

Figure 3. Real part, $\chi'_M(\omega,T)$, of the frequency-dependent susceptibility of the hydration shells of thickness 6 (squares) and 12 Å (circles). The calculations based on the time correlation function of the shell dipole moment are done at $\nu = \omega/(2\pi) = 1$ GHz (open points) and 10 GHz (closed points). Dashed lines are fits through the simulation points to functions of the form: $\chi'_M(\omega,T) = (A_1 + A_2/T)/(1 + (\omega\tau(T))^2)$ with adjustable amplitudes A_i and an Arrhenius relaxation time $\tau(T) = \tau_0 e^{H/T}$, in which τ_0 and H are fitting parameters as well.

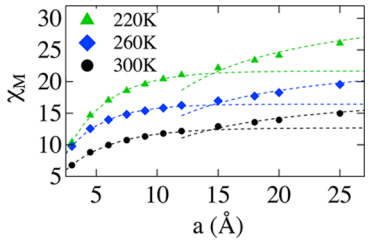

Figure 4. $\chi^M(a)$ at different temperatures indicated in the plot. The dependence on the shell thickness has a clear crossover at $a_d \simeq 12-15$ Å. The lines through the simulation points are fits to the function $\propto (1 - \exp[-a/\Lambda_d])$, $\Lambda_d \simeq 3-6$ Å at $a < a_d$ and to the function $A_1 - A_2/a$ at $a > a_d$.

The relaxation time $\tau_M(a,T)$ shows a clear crossover between two approximately Arrhenius dependences at the temperature of the dynamic freezing of the hydration shell of thickness a. The activation enthalpy H_a of the dipolar relaxation is significantly lower at high temperatures ($H_a \simeq 0.5$ kcal/mol) than below the dynamical freezing crossover ($H_a \simeq 5$ kcal/mol). The magnitude of the high-temperature activation energy is also noticeably lower than the activation energy characterizing the α-relaxation of bulk water ($H_a(\tau_D) \simeq 2.7$ kcal/mol,[35] τ_D is the Debye relaxation time). This observation, which is in agreement with simulations of the Stokes-shift dynamics,[33] indicates a structurally softer hydration shell compared with bulk water. Many relaxation processes in proteins, including displacements of the heme iron reported by Mössbauer spectroscopy[36] and electron transfer reactions,[37] are mostly affected by the hydration shell instead of the bulk. The shell relaxation time is therefore a better representation of the dynamics recorded by these observations. We also note that the dynamics of the shell density are distinctly different from the dynamics of the dipole moment. The average relaxation time, τ_N, obtained from $C_N(t) = \langle \delta N_s(t)\delta N_s(0)\rangle$ analogously to eq 2, displays an anti-Arrhenius temperature dependence with the negative activation enthalpy of $H_a = -0.9$ kcal/mol (Figure S3 in SI): a density perturbation of a less compressible shell at a low temperature relaxes faster. We find no crossover temperature in $\tau_N(T)$, in contrast with $\tau_M(T)$.

Figure 2c shows that the hydration layers closer to the protein are on average slower than the layers including more water molecules.[38] In particular, the first-shell dipole moment ($a = 3$ Å) relaxes on the time scale of ≃0.7 ns at 300 K. These collective dynamics are significantly slower than one-particle rotational dynamics of water molecules in the bulk (≃ 2.6 ps relaxation time[39]) and corresponding one-particle rotational dynamics near molecular solutes.[38] The relaxation times of small and large shells converge below the dynamical freezing temperature (glass transition). Large-scale elastic motions of the protein become inactive below this temperature and, with them, the displacements of polarized surface domains induced by the protein elasticity.[40]

The dependence of the dipolar susceptibility $\chi_M(a)$ on the shell thickness a is shown in Figure 4. We have found a clear crossover between two regions. The susceptibility saturates below the crossover distance $a_d \simeq 12-15$ Å. The distance dependence in this range fits well to an exponential function $\propto(1 - \exp[-a/\Lambda_d(T)])$ with the correlation length $\Lambda_d(T) \simeq$ 3−6 Å, which is fairly insensitive to temperature. The saturation plateau is followed at $a > a_d$ by another slow increase in $\chi_M(a)$. The following reasoning explains this observation.

Assume the dipole moment of the hydration shell separated into the dipole moment of the nanodomain $\mathbf{M}_d$ and the dipole moment of the remaining bulk water $\mathbf{M}_w$. When the thickness a is below the thickness of the domain a_d, the susceptibility grows exponentially with increasing a, as expected for highly correlated media.[3] The corresponding correlation length is Λ_d. When $a > a_d$, fluctuations of the bulk water dipoles add to the variance of the complete domain $\langle(\delta M_d)^2\rangle$. The bulk dipoles are much less correlated than the domain dipoles and the variance $\langle(\delta M_w)^2\rangle$ scales, to a first approximation, as the number of uncorrelated waters (Poisson noise): $\langle(\delta M_w)^2\rangle \propto (\langle N_s(a)\rangle - \langle N_d\rangle)$, where $\langle N_d\rangle$ is the average number of waters in the nanodomain. Therefore, the susceptibility at $a > a_d$ takes the form

$$\chi_M \simeq \chi_d + \left(1 - \frac{\langle N_d\rangle}{\langle N_s(a)\rangle}\right)\chi_w \qquad (3)$$

where χ_d and χ_w are the nanodomain and bulk water susceptibilities, respectively. Our analysis shows that $\langle N_s(a)\rangle$ scales approximately linearly with a at $a > a_d$ (Figure S4 in SI). One therefore anticipates a a^{-1} scaling in the second summand in eq 3. This expectation is supported by the calculations: $\chi_M(a)$ fits well to the generic form $A_1 - A_2/a$ at $a > a_d$ (Figure 4). The important outcome of this analysis is an estimate of the depth of the dipolar nanodomain, $a_d \simeq 12-15$ Å. We also find that this length is nearly temperature-independent and is likely determined by the distribution of the protein surface charge.

The slow, relative to the bulk, dynamics of dipolar nanodomains offer an intriguing opportunity for the dynamical control of reactions catalyzed by proteins.[41] Fast reactions and relaxation events occurring in protein active sites (such as, for instance, electronic transitions changing its oxidation state[42]) will effectively "see" hydration shells made of polarized domains characterized by a net dipole moment. This net polarization, existing only on the time scales shorter than the domain's relaxation time, will affect the energetics of the catalyzed reaction. However, the shell polarization will average to zero for slower reactions occurring on time scales longer than the time of domain relaxation. The energetics of these slower reactions will be different from the energetics of faster reactions, with a possibility of a dynamics-controlled switch between the two regimes.[42]

Our focus here is on the depth of the hydration layer perturbed by the protein. There is, however, another side to the effect of the protein−water interface related to the propagation

DOI: 10.1021/jz5025433
J. Phys. Chem. Lett. 2015, 6, 407−412

of the interfacial perturbation into the protein interior. The interior groups get more mobile with increasing hydration,[43] and larger volumes become available for a single-well diffusion of the interior atoms.[44] The enhanced vibrational softness might be partially caused by electrostatics. In this scenario, the interface will extend in two opposite directions from the dividing surface: into bulk water and into the protein interior.

■ ASSOCIATED CONTENT

Supporting Information

Simulation protocols and calculation procedures for the dipole moment of hydration shells of lysozyme. This material is available free of charge via the Internet at http://pubs.acs.org.

■ AUTHOR INFORMATION

Corresponding Author

*E-mail: dmitrym@asu.edu.

Notes

The authors declare no competing financial interest.

■ ACKNOWLEDGMENTS

This research was supported by the National Science Foundation (CHE-1213288). CPU time was provided by the National Science Foundation through XSEDE resources (TG-MCB080116N).

■ REFERENCES

(1) Phillips, G. N.; Pettitt, B. M. Structure and Dynamics of the Water Around Myoglobin. *Protein Sci.* **1995**, *4*, 149−158.

(2) Vugmaister, B. E.; Glinchuk, M. D. Dipole Glass and Ferroelectricity in Random-Site Electric Dipole Systems. *Rev. Mod. Phys.* **1990**, *62*, 993.

(3) Samara, G. A. The Relaxational Properties of Compositionally Disordered ABO_3 Perovskites. *J. Phys.: Condens. Matter* **2003**, *15*, R367−R411.

(4) Demmel, F.; Doster, W.; Petry, W.; Schulte, A. Vibrational Frequency Shift as a Probe of Hydrogen Bonds: Thermal Expansion and Glass Transition of Myoglobin in Mixed Solvents. *Eur. Biophys. J.* **1997**, *26*, 327−335.

(5) Badger, J. Multiple Hydration Layers in Cubic Insulin Crystals. *Biophys. J.* **1993**, *65*, 1656−1659.

(6) Pizzitutti, F.; Marchi, M.; Sterpone, F.; Rossky, P. J. How Protein Surfaces Induce Anomalous Dynamics of Hydration Water. *J. Phys. Chem. B* **2007**, *111*, 7584−7590.

(7) Cheng, Y.-K.; Rossky, P. J. Surface Topography Dependence of Biomolecular Hydrophobic Hydration. *Nature* **1998**, *392*, 696−699.

(8) Godec, A.; Smith, J. C.; Merzel, F. Increase of both Order and Disorder in the First Hydration Shell with Increasing Solute Polarity. *Phys. Rev. Lett.* **2011**, *107*, 267801.

(9) Lee, C. Y.; McCammon, J. A.; Rossky, P. J. The Structure of Liquid Water at an Extended Hydrophobic Surface. *J. Chem. Phys.* **1984**, *80*, 4448−4455.

(10) Smith, J. C.; Merzel, F.; Bondar, A. N.; Tournier, A.; Fischer, S. Structure, Dynamics and Reactions of Protein Hydration Water. *Philos. Trans. R. Soc., B* **2004**, *359*, 1181−1190.

(11) Mondal, J. A.; Nihonyanagi, S.; Yamaguchi, S.; Tahara, T. Three Distinct Water Structures at a Zwitterionic Lipid/Water Interface Revealed by Heterodyne-Detected Vibrational Sum Frequency Generation. *J. Am. Chem. Soc.* **2012**, *134*, 7842−7850.

(12) Ball, P. Water as an Active Constituent in Cell Biology. *Chem. Rev.* **2008**, *108*, 74.

(13) Friesen, A. D.; Matyushov, D. V. Surface Polarity and Nanoscale Solvation. *J. Phys. Chem. Lett.* **2012**, *3*, 3685−3689.

(14) Friesen, A. D.; Matyushov, D. V. Non-Gaussian Statistics of Electrostatic Fluctuations of Hydration Shells. *J. Chem. Phys.* **2011**, *135*, 104501.

(15) Umezawa, K.; Higo, J.; Shimotakahara, S.; Shindo, H. Collective Solvent Flows around a Protein Investigated by Molecular Dynamics Simulation. *J. Chem. Phys.* **2007**, *127*, 045101.

(16) LeBard, D. N.; Matyushov, D. V. Ferroelectric Hydration Shells around Proteins: Electrostatics of the Protein-Water Interface. *J. Phys. Chem. B* **2010**, *114*, 9246−9258.

(17) Nakanishi, M.; Sokolov, A. P. Protein Dynamics in a Broad Frequency Range: Dielectric Spectroscopy Studies. *J. Non-Cryst. Solids* **2014**, *407*, 478−485.

(18) Bagchi, K.; Roy, S. Sensitivity of Water Dynamics to Biologically Significant Surfaces of Monomeric Insulin: Role of Topology and Electrostatic Interactions. *J. Phys. Chem. B* **2014**, *118*, 3805−3813.

(19) Sterpone, F.; Stirnemann, G.; Laage, D. Magnitude and Molecular Origin of Water Slowdown Next to a Protein. *J. Am. Chem. Soc.* **2012**, *134*, 4116−4119.

(20) Stirnemann, G.; Castrillon, S. R.-V.; Hynes, J. T.; Rossky, P. J.; Debenedetti, P. G.; Laage, D. Non-Monotonic Dependence of Water Reorientation Dynamics on Surface Hydrophilicity: Competing Effects of the Hydration Structure and Hydrogen-Bond Strength. *Phys. Chem. Chem. Phys.* **2011**, *13*, 19911−19917.

(21) Svergun, D. I.; Richard, S.; Koch, M. H. J.; Sayers, Z.; Kuprin, S.; Zaccai, G. Protein Hydration in Solution: Experimental Observation by X-ray and Neutron Scattering. *Proc. Natl. Acad. Sci. U. S. A.* **1998**, *95*, 2267−2272.

(22) Heyden, M.; Bründermann, E.; Heugen, U.; Leitner, D. M.; Havenith, M. Long-Range Influence of Carbohydrates on the Solvation Dynamics of Water − Answers from Terahertz Absorption Measurements and Molecular Modeling Simulations. *J. Am. Chem. Soc.* **2008**, *130*, 5773−5779.

(23) Matyushov, D. V. Dipolar Response of Hydrated Proteins. *J. Chem. Phys.* **2012**, *136*, 085102.

(24) Gekle, S.; Netz, R. R. Anisotropy in the Dielectric Spectrum of Hydration Water and its Relation to Water Dynamics. *J. Chem. Phys.* **2012**, *137*, 104704−12.

(25) Zhang, C.; Gygi, F.; Galli, G. Strongly Anisotropic Dielectric Relaxation of Water at the Nanoscale. *J. Phys. Chem. Lett.* **2013**, *4*, 2477−2481.

(26) Jordanides, X. J.; Lang, M. J.; Song, X.; Fleming, G. R. Solvation Dynamics in Protein Environments Studied by Photon Echo Spectroscopy. *J. Phys. Chem. B* **1999**, *103*, 7995.

(27) Schirò, G.; Fomina, M.; Cupane, A. Communication: Protein Dynamical Transition vs. Liquid-Liquid Phase Transition in Protein Hydration Water. *J. Chem. Phys.* **2013**, *139*, 121102.

(28) Phillips, J. C.; Braun, R.; Wang, W.; Gumbart, J.; Tajkhorshid, E.; Villa, E.; Chipot, C.; Skeel, R. D.; Kale, L.; Schulten, K. Scalable Molecular Dynamics with NAMD. *J. Comput. Chem.* **2005**, *26*, 1781−1802.

(29) Perera, P. N.; Fega, K. R.; Lawrence, C.; Sundstrom, E. J.; Tomlinson-Phillips, J.; Ben-Amotz, D. Observation of Water Dangling OH Bonds around Dissolved Nonpolar Groups. *Proc. Natl. Acad. Sci. U.S.A.* **2009**, *106*, 12230−12234.

(30) Matyushov, D. V. Electrophoretic Mobility without Charge Driven by Polarisation of the Nanoparticle−Water Interface. *Mol. Phys.* **2014**, *112*, 2029−2039.

(31) Remsing, R. C.; Baer, M. D.; Schenter, G. K.; Mundy, C. J.; Weeks, J. D. The Role of Broken Symmetry in Solvation of a Spherical Cavity in Classical and Quantum Water Models. *J. Phys. Chem. Lett.* **2014**, *5*, 2767−2774.

(32) Böttcher, C. J. F. *Theory of Electric Polarization*; Elsevier: Amsterdam, 1973; Vol. *1*.

(33) LeBard, D. N.; Matyushov, D. V. Dynamical Transition, Hydrophobic Interface, and the Temperature Dependence of Electrostatic Fluctuations in Proteins. *Phys. Rev. E* **2008**, *78*, 061901.

(34) Barlow, D. J.; Thornton, J. M. Charge Distribution in Proteins. *Biopolymers* **1986**, *25*, 1717−1733.

(35) Bertolini, D.; Cassettari, M.; Salvetti, G. The Dielectric Relaxation Time of Supercooled Water. *J. Chem. Phys.* **1982**, *76*, 3285.

(36) Frauenfelder, H.; Chen, G.; Berendzen, J.; Fenimore, P. W.; Jansson, H.; McMahon, B. H.; Stroe, I. R.; Swenson, J.; Young, R. D. A

DOI: 10.1021/jz5025433
J. Phys. Chem. Lett. 2015, 6, 407−412

Unified Model of Protein Dynamics. *Proc. Natl. Acad. Sci. U. S. A.* **2009**, *106*, 5129−5134.
(37) Matyushov, D. V. Nanosecond Stokes Shift Dynamics, Dynamical Transition, and Gigantic Reorganization Energy of Hydrated Heme Proteins. *J. Phys. Chem. B* **2011**, *115*, 10715−10724.
(38) Laage, D.; Stirnemann, G.; Sterpone, F.; Rey, R.; Hynes, J. T. Reorientation and Allied Dynamics in Water and Aqueous Solutions. *Annu. Rev. Phys. Chem.* **2011**, *62*, 395−416.
(39) Tielrooij, K. J.; Garcia-Araez, N.; Bonn, M.; Bakker, H. J. Cooperativity in Ion Hydration. *Science* **2010**, *328*, 1006−1009.
(40) Martin, D. R.; Matyushov, D. V. Non-Gaussian Statistics and Nanosecond Dynamics of Electrostatic Fluctuations Affecting Optical Transitions in a Green Fluorescent Protein. *J. Phys. Chem. B* **2012**, *116*, 10294−10300.
(41) Henzler-Wildman, K. A.; Thai, V.; Lei, M.; Ott, M.; Wolf-Watz, M.; Fenn, T.; Pozharski, E.; Wilson, M. A.; Petsko, G. A.; Karplus, M.; et al. Intrinsic Motions along an Enzymatic Reaction Trajectory. *Nature* **2007**, *450*, 838−844.
(42) LeBard, D. N.; Martin, D. R.; Lin, S.; Woodbury, N. W.; Matyushov, D. V. Protein Dynamics to Optimize and Control Bacterial Photosynthesis. *Chem. Sci.* **2013**, *4*, 4127−4136.
(43) Zanotti, J.-M.; Bellissent-Funel, M.-C.; Parello, J. Hydration-Coupled Dynamics in Proteins Studied by Neutron Scattering and NMR: The Case of the Typical EF-Hand Calcium-Binding Parvalbumin. *Biophys. J.* **1999**, *76*, 2390−2411.
(44) Hong, L.; Cheng, X.; Glass, D.; Smith, J. Surface Hydration Amplifies Single-Well Protein Atom Diffusion Propagating into the Macromolecular Core. *Phys. Rev. Lett.* **2012**, *108*, 238102.

DOI: 10.1021/jz5025433
J. Phys. Chem. Lett. 2015, 6, 407−412